

present in solution. In spite of these precautions, we cannot completely exclude the possibility that the formation of this paramagnetic product in this reaction and its possible inadvertent inclusion into polyethylene could account for the residual ESR signal seen in Figure 2 since ESR is such a sensitive technique.

- (16) A diastereomer of dithioerythritol, dithiothreitol, is known to act as a reducing agent toward nitroxyl radicals: cf. Keana, J. F. W. *Chem. Rev.* **1978**, *78*, 37-64.
- (17) Several literature reports describe reduction of nitroxyl radicals by hydrazine derivatives: cf. Keana, J. F. W.; Lee, T. D.

*J. Org. Chem.* **1975**, *40*, 3145-3147. Daniel, W. E., Jr.; Cohn, M. *Biochemistry* **1976**, *15*, 3917-3924. Rozantsev, E. G. "Free Nitroxyl Radicals"; Plenum Press: New York, 1970; Chapter 4.

- (18) Examples of use of sodium ascorbate to reduce nitroxyl groups include ref 13 and Kornberg et al. (Kornberg, R. D.; McConnell, H. M. *Biochemistry* **1971**, *10*, 1111-1120).
- (19) Reduction of nitroxyl radicals by sodium sulfide in dimethylformamide is preceded: cf. Kornblum, N.; Pinnick, H. W. *J. Org. Chem.* **1972**, *37*, 2050-2051.
- (20) Tomboulou, P. *J. Org. Chem.* **1959**, *24*, 229-234.

## Excited-State Annihilation Processes in Poly(vinylaromatics) in Solution: Poly(2-vinylnaphthalene) and Poly(4-vinylbiphenyl)

James F. Pratte<sup>†</sup> and Stephen E. Webber\*

Department of Chemistry and Center for Polymer Research, University of Texas at Austin, Austin, Texas 78712. Received November 18, 1983

**ABSTRACT:** The triplet yield (measured by T-T absorption) and monomer and excimer fluorescence (measured from integrated intensities) have been determined as a function of laser intensity using a Nd:YAG Q-switched laser at 266 nm for the title polymers. At higher laser intensities the polymer triplet yield and fluorescence tended to saturate to a much greater extent than monomeric model compounds (i.e., naphthalene or 4-methylbiphenyl). This is interpreted to be the result of S-S and S-T intracoincidence annihilation, which appears to be much more important in polymer photophysics than is usually the case with small molecules in solution. It was also observed that in CH<sub>2</sub>Cl<sub>2</sub> solvent (but not methyltetrahydrofuran) the S-S annihilation leads to radical cation formation of the pendent aromatic by virtue of electron capture by the solvent. The implication of these results with respect to general photophysical and energy migration processes in polymers is discussed.

### Introduction

In an earlier report the triplet quantum yield of poly(2-vinylnaphthalene) (P2VN) was found to be very low and inversely proportional to the molecular weight.<sup>1</sup> It was postulated that the reduction of the triplet quantum yield relative to the monomeric model compound was the result of singlet excimer formation. But the magnitude of this reduction and the inverse molecular weight effect on the triplet quantum yield left some puzzling questions. There have been other reports of low triplet quantum yields in polymers by Masuhara et al.<sup>2</sup> for carbazole- and pyrene-containing polymers, by Lachish and Williams for poly(vinylcarbazole) (PVCz),<sup>3</sup> and by Gupta et al.<sup>4</sup> for poly(1-vinylnaphthalene) (P1VN). Masuhara et al.<sup>2a</sup> concluded that the reason for the low triplet yield in polymers of PVCz was singlet-singlet annihilation of excitons on the same polymer chain. Thus, the present study was designed to reexamine P2VN and also to understand the general features of singlet-singlet annihilation in poly(vinylaromatic) polymers.

### Experimental Section

The synthesis and characterization of P2VN and P4VBP have been described previously.<sup>5-7</sup> The numeration of the polymers is the same as those used in previous experiments. 1,3-ββ-Dinaphthylpropane (DNP) was the same material as in an earlier report.<sup>8</sup> 2-Methyltetrahydrofuran (MTHF) was purchased from Aldrich Chemicals. MTHF was filtered through freshly activated alumina and refluxed over lithium aluminum hydride under a nitrogen atmosphere before use. Dichloromethane (spectrograde MCB and Fisher), cyclohexane (spectroquality MCB), isooctane (Gold Label Aldrich 99%), and chloroform (spectroquality MCB) were used as received. Naphthalene (Aldrich) was sodium fused and then a gradient sublimation was performed. 2-Ethyl-naphthalene (Aldrich 99+%) was used as received while 4-

methylbiphenyl (Aldrich 98%) was recrystallized several times from methanol and then chromatographed on alumina using hexane as the eluent.

The laser flash photolysis unit was the same as that used previously<sup>7</sup> at the Center for Fast Kinetics Research, University of Texas at Austin. A Q-switched Quantel 481-Nd:YAG laser (λ 266 nm, 70 mJ, 11-ns pulse width) was used as the excitation source. The laser beam is circular (8-10 mm in diameter) and the intensity profile is approximately Gaussian. Optical alignment for this experiment was a cross beam arrangement in which the excitation beam is 90° to the monitoring beam provided by a 150-W xenon lamp that was powered by a PRA Model 303 lamp supply. The monitoring beam could also be pulsed by a PRA Model 305 pulser which produces a more intense interrogation light source with essentially constant intensity for up to 20 μs. A cylindrical lens is used to direct most of the laser light into an image parallel to the direction of the monitoring beam. The monitoring beam sampled the first millimeter of the side of the cuvette toward the laser beam. The path length of the cuvettes used in these experiments was 1 cm. Solutions used in the intensity dependence studies and triplet quantum yield measurement had optical densities of 0.5 at the laser wavelength while for the transient spectra the optical density was 1.5 at λ<sub>ex</sub>. Naphthalene in cyclohexane<sup>9</sup> was used as the standard in the measurement of the triplet quantum yield and also as the relative actinometer in determining the average photon flux over the path length of the cuvette using the relation derived by Bensasson et al.<sup>10</sup> It should be stressed that our calculated values for the laser intensity are averaged over the spatial inhomogeneity of the laser beam across the path length of the cuvette.

Signals for the absorption experiments were captured with a Biomation 8100 transient recorder while for the emission experiments a Tektronix 7912 digitizer was used. The signal traces were then transferred to a PDP 11/70 computer where the data were stored and processed. Time-resolved absorption spectra were obtained by assembling decay curves at every 5 or 10 nm. The integrated fluorescence values (I<sub>F</sub>) were obtained by integrating the area underneath the decay curve of the emission taken from the same optical alignment as the absorption with the monitoring beam turned off.

<sup>†</sup> Present address: E. I. du Pont, Wilmington, DE.

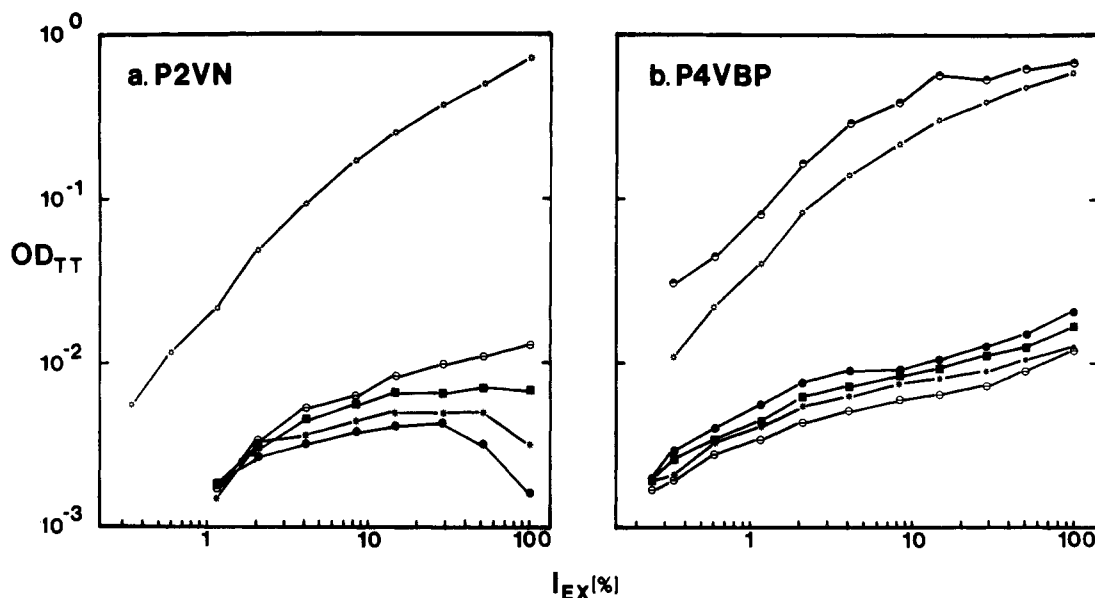


**Figure 1.** (a) Maximum OD<sub>TT</sub> ( $\lambda_{\text{obsd}}$  427 nm) for P2VN samples in MTHF and naphthalene ( $\lambda_{\text{obsd}}$  414 nm) in cyclohexane ( $\star$ ) as a function of laser intensity (%). The symbols are as follows:  $\ominus$ , 1 ( $P = 167$ );  $\star$ , 2 ( $P = 346$ );  $\blacksquare$ , 3 ( $P = 883$ );  $\bullet$ , 4 ( $P = 2806$ ). (b) Maximum OD<sub>TT</sub> (380 nm) for P4VBP in MTHF and naphthalene ( $\star$ ) in cyclohexane and 4-methylbiphenyl ( $\bullet$ ) in cyclohexane. The symbols are as follows:  $\ominus$ , 1 ( $P = 149$ );  $\star$ , 2 ( $P = 249$ );  $\blacksquare$ , 3 ( $P = 437$ );  $\bullet$ , 4 ( $P = 1236$ ). For 100% the photon/cm<sup>2</sup> per shot was estimated as  $5.5 \times 10^{16}$  for P2VN and  $1 \times 10^{17}$  for P4VBP.

A Spex Fluorolog (Model 1902) fluorometer was used to record steady-state fluorescence spectra. Naphthalene in cyclohexane<sup>11</sup> was used as the standard in the measurement of the fluorescent quantum yield ( $\Phi_f$ ) for naphthalenic compounds while 4-methylbiphenyl in cyclohexane<sup>11</sup> was the standard in the measurement of  $\Phi_f$  for P4VBP. Fluorescent lifetimes were recorded with a mode-locked Quantel Nd:YAG laser ( $\lambda$  265 nm, 5 mJ, 40-ps pulse width) along with the Tektronix 7912 digitizer.

## Results

**(a) Laser Intensity Dependence of Triplet Formation.** In the earlier report<sup>1</sup> of the triplet yield of P2VN it was observed that  $\Phi_{\text{isc}}^{\text{polym}} \ll \Phi_{\text{isc}}^{\text{model}}$  (the model compound used was 2-ethylnaphthalene). In addition  $\Phi_{\text{isc}}^{\text{polym}}$  was found to decrease with increasing molecular weight. In Figure 1a is presented a plot of the optical density of T-T absorption for naphthalene in cyclohexane and the various P2VN polymers in MTHF (see Table I for relevant properties). While it is certainly the case that  $\Phi_{\text{isc}}^{\text{polym}} \ll \Phi_{\text{isc}}^{\text{model}}$ , the difference is decreased radically in the low  $I_{\text{ex}}$  limit ( $I_{\text{ex}}$  = photons/cm<sup>2</sup> per laser shot). Furthermore the deviation from a linear dependence on  $I_{\text{ex}}$  in the case of the polymer is striking and depends on the molecular weight of the polymer. It is this effect that leads to the apparent molecular weight effects reported previously. We note here that the monomer to excimer ratio in fluorescence spectra is essentially identical for this series, which we will argue later implies that photon absorption by the excimer state (i.e., successive two-photon absorption) is not responsible for these nonlinearities.

For laser intensities above 20% the naphthalene standard begins to display a nonlinear dependence on  $I_{\text{ex}}$ , which can result from ground-state bleaching and/or inner-filter effects from excited-state transient absorption.<sup>12</sup> The  $I_{\text{ex}}$  dependence  $\Phi_{\text{isc}}^{\text{polym}}$  is remarkably nonlinear, approaching  $I_{\text{ex}}^{-1}$  for the highest laser intensities and highest molecular weights. Clearly, saturation or excited-state annihilation is much more important for the polymer than the monomeric model compounds, and this process increases in importance as the degree of polymerization increases.

In Figure 1b are presented analogous results for poly(4-vinylbiphenyl) (P4VBP) in MTHF. Even at the lowest

**Table I**  
Photophysical Constants of Polymers and Model Compounds

compound	solvent	$P^a$	$\Phi_{\text{isc}}$	$\Phi_f$
P2VN-1	MTHF	167	0.12	0.12
P2VN-2	MTHF	346	0.12	0.12
P2VN-3	MTHF	883	0.10	0.13
P2VN-4	MTHF	2806	0.13	0.14
naphthalene	cyclohexane		0.75 <sup>b</sup>	0.23 <sup>c</sup>
2-methylnaphthalene	cyclohexane		0.56 <sup>b</sup>	0.32 <sup>c</sup>
DNP	isooctane	2	0.42	0.16
P4VBP-1	MTHF	149	0.15	0.38
P4VBP-2	MTHF	249	0.15	0.38
P4VBP-3	MTHF	437	0.15	0.40
P4VBP-4	MTHF	1236	0.15	0.38
4-methylbiphenyl	cyclohexane		0.84 <sup>b</sup>	0.17 <sup>c</sup>
biphenyl	cyclohexane		0.84 <sup>b</sup>	0.18 <sup>c</sup>

<sup>a</sup> Degree of polymerization =  $P$ . The values for P2VN have been multiplied by 2 to correct the mistake made in ref 5. <sup>b</sup> Bensasson, R.; Amand, B. *Chem. Phys. Lett.* 1975, 34, 44. <sup>c</sup> Berlman, I. B. "Handbook of Fluorescent Spectra of Aromatic Molecules", 2nd ed.; Academic Press: New York, 1971.

$I_{\text{ex}}$  values for which a significant optical density of biphenyl triplet could be measured ( $\lambda_{\text{obsd}}$  380 nm) the optical density has a sublinear  $I_{\text{ex}}$  dependence. While there is an inverse molecular weight effect at higher  $I_{\text{ex}}$  values, it does not seem to be exaggerated at the highest  $I_{\text{ex}}$  values as is the case for P2VN. Also for these polymers the yield of triplet seems to actually increase slightly at the highest intensities after having nearly saturated at intermediate intensities. Note that the triplet absorption of the naphthalene standard and 4-methylbiphenyl remains linear in  $I_{\text{ex}}$  up to  $\sim 10\%$  full intensity for this set of experiments.

The transient absorption behavior of these two polymer systems is completely different if the solvent system is changed to CH<sub>2</sub>Cl<sub>2</sub>. While the transient absorption spectrum in MTHF is clearly that of the T<sub>1</sub> state, in CH<sub>2</sub>Cl<sub>2</sub> the transient spectra most nearly resemble the radical cation spectra seen in Irie et al.<sup>13</sup> and Arai et al.<sup>14</sup> (see Figure 2). Unfortunately, the optical density at low laser intensities was too small to obtain a good quality transient absorption spectrum such that a direct determination of the presence of a species other than radical

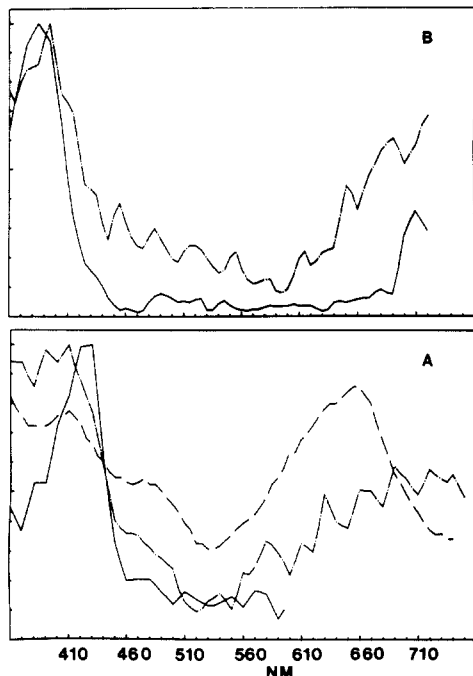


**Figure 2.** (a) Transient absorption spectrum of P2VN-1 in MTHF (—) and  $\text{CH}_2\text{Cl}_2$  (---). The P2VN radical cation spectrum reported by Irie et al.<sup>13</sup> is also shown for comparison (-.-). (b) P4VBP-1 in MTHF (—) and  $\text{CH}_2\text{Cl}_2$  (---).

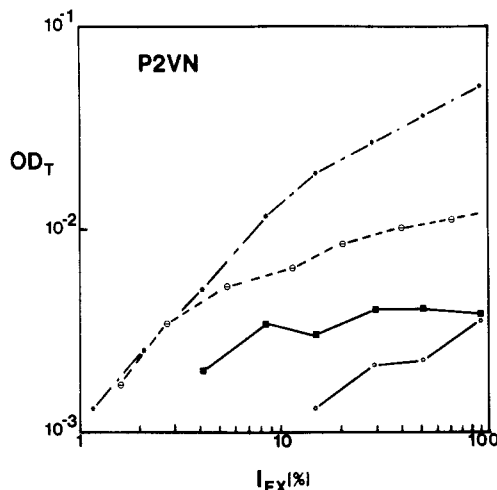


**Figure 3.** Log-log plot of the fast (■) and slow (☆) components of  $\text{OD}_T^{\max}$  vs.  $I_{\text{ex}}$  for P2VN in  $\text{CH}_2\text{Cl}_2$  at  $\lambda_{\text{obs}} = 427$  nm in the presence of  $\text{O}_2$  (see text). The displaced curves for P2VN-1 in MTHF (○) and naphthalene in cyclohexane (★) from Figure 1a are shown for comparison.

cation was impossible. However, the following experiment does suggest that there is competitive formation of the  $T_1$  state and the  $M^+$  radical cation. The  $T_1$  lifetime is greatly shortened by  $\text{O}_2$  quenching while that of  $M^+$  is virtually unaffected. Thus if the transient optical density is monitored at 427 nm where both  $T_1$  and  $M^+$  absorb, the decay of the optical density becomes strongly biexponential upon admission of  $\text{O}_2$  while at 650 nm (absorption by  $M^+$  only) there is essentially no change. Thus at 427 nm the transient optical density can be interpreted as

$$\text{OD}_T(t) = \epsilon_{T_1}[T_1] \exp(-k_{T_1}t) + \epsilon_{M^+}[M^+] \exp(-k_{M^+}t) \quad (1)$$

where  $\epsilon_{M^+}[M^+]$  is the intercept of the slow component of  $\text{OD}_T(t)$  at  $t = 0$  and  $\epsilon_{T_1}[T_1]$  is found by difference. These data are plotted in Figure 3 for P2VN and clearly demonstrate the relative enhancement of  $[M^+]$  as  $I_{\text{ex}}$  increases. We note that the  $T_1$  (fast) component displays saturation

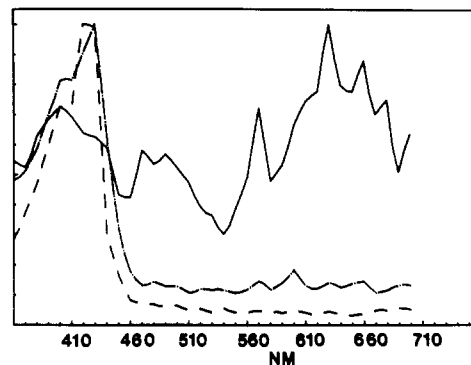


**Figure 4.** Transient absorption spectrum of naphthalene (---),  $\beta,\beta$ -dinaphthylpropane (-.-), and P2VN-1 (—) in  $\text{CH}_2\text{Cl}_2$  at high laser intensity ( $I_{\text{ex}} = 4 \times 10^{16}$  photons/ $\text{cm}^2$  of full power).

behavior like that for P2VN-1 in MTHF (replotted from Figure 1a for comparison). Biexponential decay was only observed for relatively high laser intensities ( $>10\%$  full power). For lower  $I_{\text{ex}}$  the transient optical density was composed only of a single rapidly decaying signal in aerated solutions, implying that only the  $T_1$  state is produced. The data for P4VBP in  $\text{CH}_2\text{Cl}_2$  (not shown) are not as revealing as the data for P2VN. However, the strongly biexponential decay at the wavelength where the triplet absorbs is also observed when  $\text{O}_2$  is admitted. Thus there are two absorbing species in the transient absorption spectrum and the relative concentration of these species depends upon the laser intensity.

An important observation concerning radical cation formation in  $\text{CH}_2\text{Cl}_2$  solutions is that at laser intensities such that the radical cation is produced for the polymer only the  $T_1$  state is found for naphthalene and/or 4-methylbiphenyl. This is illustrated in Figure 4 for the naphthalene compounds. The relative ratio of triplet to radical cation increases in the following order: naphthalene  $>$  DNP  $>$  P2VN. Note that DNP exhibits facile excimer formation, such that the importance of a successive two-photon absorption process  $S_0 \rightarrow {}^1D^* \rightarrow {}^1M^{**}$  should be similar for DNP and P2VN. Thus, we conclude that production of the radical cation requires the juxtaposition of two excited states.

**(b) Laser Intensity Dependence of Monomer and Excimer Fluorescence.** As mentioned in the Introduction, Masuhara and co-workers have postulated S-S annihilation to be the origin of lowered triplet quantum yields in PVCz.<sup>2</sup> We have tested this idea by measuring the integrated monomer and excimer fluorescence intensity of our polymer systems under exactly the same experimental conditions as the T-T absorption experiments. While no important molecular weight effects or solvent dependencies were observed for either polymer, both monomer and excimer fluorescence intensities were sub-linear in  $I_{\text{ex}}$  at laser intensities for which the monomeric model compounds were linear in  $I_{\text{ex}}$  (see Figure 5). There was also a substantial difference in the  $I_{\text{ex}}$  dependence of the monomer and excimer fluorescence, with the latter tending to saturate well before the former. The fluorescence data for the P2VN and P4VBP systems are remarkably similar (i.e., cf. Figure 5a,b).

Thus the important experimental findings are the following:

(1) The production of excited states in P2VN and P4VBP tends to be sublinear in laser intensity under conditions where a monomeric model compound is still linear. The degree of nonlinearity increases in the (approximate) order  ${}^1M^* < {}^1D^* \leq T_1$ , where  ${}^1M^*$  and  ${}^1D^*$  refer to excited polymer monomer and excimer singlet states,

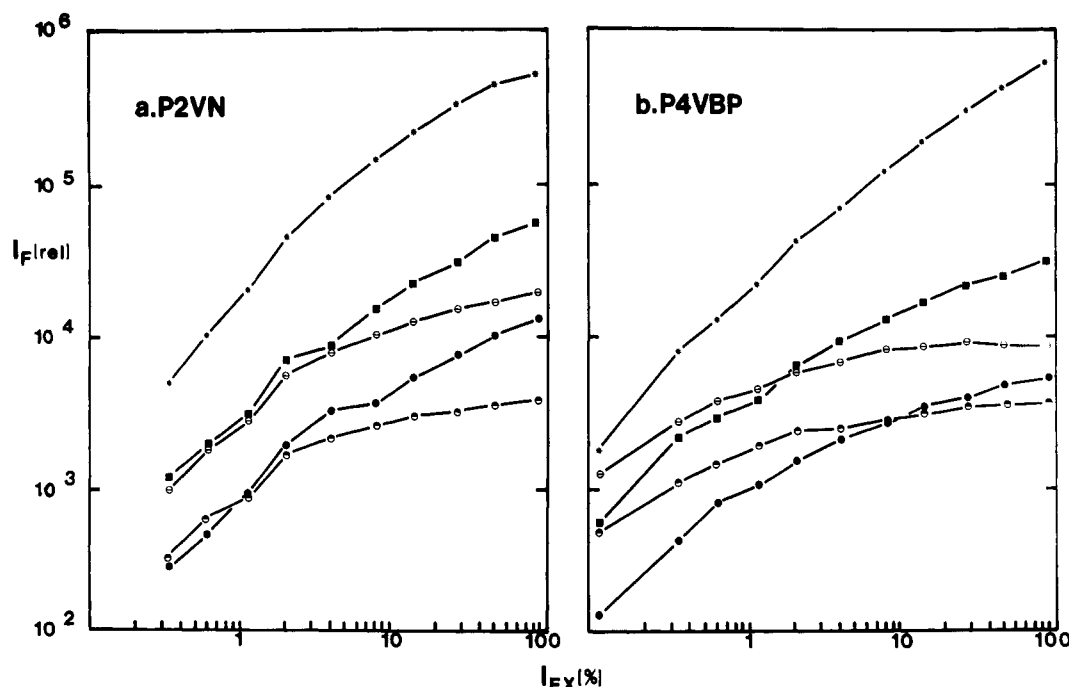


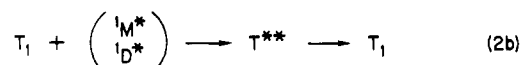
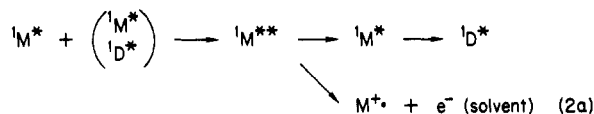
**Figure 5.** (a) Integrated fluorescence intensity for monomer (■, ●,  $\lambda_{\text{obsd}}$  325 nm) in MTHF and  $\text{CH}_2\text{Cl}_2$ , respectively, and excimer (○, ◐,  $\lambda_{\text{obsd}}$  440 nm) in MTHF and  $\text{CH}_2\text{Cl}_2$ , respectively, for P2VN-1. (b) Integrated fluorescence intensity for monomer (■, ●,  $\lambda_{\text{obsd}}$  315 nm) in MTHF and  $\text{CH}_2\text{Cl}_2$ , respectively, and excimer (○, ◐,  $\lambda_{\text{obsd}}$  400 nm) in MTHF and  $\text{CH}_2\text{Cl}_2$ , respectively, for P4VBP-1. For both plots ★ is the integrated fluorescence intensity of naphthalene in cyclohexane. There was no significant difference between different P2VN or P4VBP samples.

respectively, and  $T_1$  is the lowest triplet state (based on the transient spectra  $T_1$  is assumed not to be an excimer state).

(2) In the case of P2VN the nonlinearity in the yield of  $T_1$  is clearly molecular weight dependent but much less so in the case of P4VBP.

(3) The relative yields of  $T_1$  and cation radical ( $M^+$ ) depend on the solvent. The cation radical is formed exclusively in  $\text{CH}_2\text{Cl}_2$  at higher laser energies.

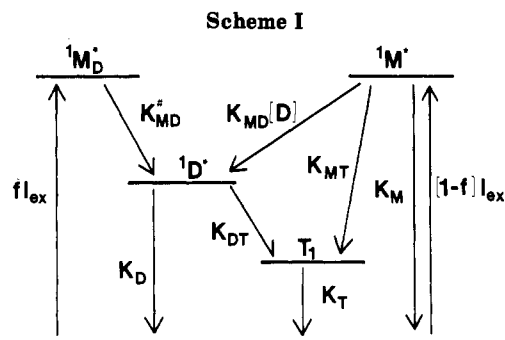
We will argue in the next section that all these observations are the result of intracoil excited-state annihilations of the following types:



These processes are complex and would be difficult to analyze even if the excitation pulse approximated either a  $\delta$ -function or steady-state conditions. However, because the pulse width of the Q-switched laser is on the order of the excited-state lifetimes, our discussion in the next section will be qualitative only. The experimental results as they stand serve to emphasize the following point with respect to polymer photophysics and spectroscopy: because of the high local density of absorbing groups and the possibility of extensive energy migration, excited-state annihilation is likely in polymer systems at photon fluxes far below those required for small molecules in solution.

## Discussion

The experimental results cited in the previous section demonstrate strong nonlinearities in the production of the  ${}^1M^*$ ,  ${}^1D^*$ , and  $T_1$  excited states as a function of the laser intensity,  $I_{\text{ex}}$ . We will confine our discussion to  $I_{\text{ex}}$  values such that the monomeric model (i.e., naphthalene or 4-



methylbiphenyl) is linear (usually at  $\leq 20\%$  of full laser intensity) which should eliminate to a first approximation "trivial" effects such as ground-state bleaching, inner-filter effects, etc. We also neglect a two-photon process of the following type:  $S_0 + h\nu \rightarrow {}^1M^* \rightarrow {}^1D^* + h\nu \rightarrow {}^1M^{**}$  on the grounds that the quantum efficiency of excimer formation is not molecular weight dependent for the polymers studied herein. This is not to say that this process is necessarily unimportant when comparing a polymer to a monomeric model compound, but the discussion in this section is directed toward a comparison of the polymeric systems only.

We will discuss our results using the simplified energy level diagram represented in Scheme I.

In this scheme it is assumed that direct excitation produces two types of  ${}^1M^*$  states. The  ${}^1M_D^*$  state is located at or near an excimer-forming site (EFS) such that the unimolecular decay rate  $k_{MD}^*$  (representing  ${}^1M_D^* \rightarrow {}^1D^*$ ) is so large that this species does not contribute to the monomer fluorescence. The  ${}^1M^*$  state is sufficiently distant from the nearest EFS that excimer formation is competitive with the other relaxation processes of the  ${}^1M^*$  state. The rate of excimer formation from  ${}^1M^*$  is written as  $k_{MD}[D]$ , where  $[D]$  is the effective concentration of EFS.

Obviously this model for treating the  ${}^1M^*$  and  ${}^1D^*$  states is greatly simplified since there will exist a distribution of

separations of initial photon absorption events and EFS. This problem has been discussed recently by Frank and co-workers<sup>15</sup> in their analysis of monomer and excimer fluorescence decay of vinylaromatic polymers. On the other hand the model in Scheme I does contain the most important element of any discussion of polymer excited states: the population of excited states is a heterogeneous population that depends on the "local conformation" of chromophores. It is also necessary to evoke this heterogeneity because the shortening of the fluorescence lifetime of  $^1M^*$  is not consistent with the decrease in the quantum yield of  $^1M^*$  fluorescence if one considers only the  $^1M^*$  and  $^1D^*$  states (see Appendix). This is typical of fluorescent systems in which there is simultaneous static and dynamic quenching.

A detailed, quantitative interpretation of our results is essentially impossible because the pulse width of the excitation source is of the order of the lifetime of the excited state. Furthermore since excited-state annihilation is considered, the lifetimes of the excited state depend on the number of photons absorbed previously. One should also take into account that the number of photons absorbed per polymer coil obeys Poisson or modified-Poisson statistics.<sup>16</sup> In what follows, we will write down classical kinetic equations and discuss the steady-state limit of these equations. We believe that this allows the main features of our data to be understood.

First consider  $^1M_D^*$ . This state is considered to have a very short lifetime because it is rapidly converted to an excimer at a nearby EFS. We assume that at high  $I_{ex}$  values we must correct the fraction of EFS by the factor  $1 - [^1D^*]/[D]_0$ , where  $[D]_0$  is the concentration of EFS in the absence of excitation and  $1 - [^1D^*]/[D]_0$  represents the saturation of these trap sites. Thus we write

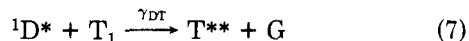
$$d[^1M_D^*]/dt = fI_{ex}(1 - [^1D^*]/[D]_0) - k_{MD}[^1M_D^*] \quad (3)$$

$$[^1M_D^*]_{ss} = fI_{ex}(1 - [^1D^*]/[D]_0)/k_{MD} \quad (4)$$

Since  $^1M_D^*$  is involved in  $^1D^*$  we now write that equation:

$$d[^1D^*]/dt = k_{MD}[^1M_D^*] + k_{MD}([D]_0 - [^1D^*])[^1M^*] - k_D[^1D^*] - \gamma_{MD}[^1M^*][^1D^*] - \gamma_{DT}[T_1][^1D^*] \quad (5)$$

In eq 5 we may substitute the steady-state result for  $^1M_D^*$  from eq 4. In the second term we have substituted  $[D]_0 - [^1D^*]$  for  $[D]$  (see Scheme I), showing that the EFS can be saturated at higher excitation energies. The following annihilation processes are considered:



The heterogeneous annihilation process in (6) is between the intracoil excimer and  $^1M^*$  exciton and requires the excited states to be within a few collision diameters of each other to occur. The S-T "annihilation" is really a Förster energy transfer process which can occur over large separations if the  $^1D^*$  fluorescence overlaps strongly with the T-T absorption. We have ignored  $^1D^* - ^1D^*$  annihilation since this excited state is immobilized. This also implies that the thermal dissociation process  $^1D^* \rightarrow ^1M^* + G$  can be ignored.

The steady-state expression for  $^1D^*$  is complicated.

$$[^1D^*]_{ss} = (fI_{ex} + k_{MD}[^1M^*]_{ss}) / (k_D + (fI_{ex}/[D]_0) + (\gamma_{MD} + k_{MD})[^1M^*]_{ss} + \gamma_{DT}[T_1]) \quad (8)$$

However, one can see that in the limit of high  $I_{ex}$  or high

$[^1M^*]_{ss}$  the value of  $[^1D^*]_{ss}$  will tend to saturate. Since the overall triplet concentration is low ( $< 1$  triplet/coil even for the highest molecular weight), it also is likely that S-T annihilation can be ignored for the  $^1D^*$  state (but not for the  $T_1$  state, as will be discussed later).

The kinetic equation for  $^1M^*$  is similar to that for  $^1D^*$  except a homogeneous annihilation term must be added, i.e.



$$d[^1M^*]/dt = (1 - f)I_{ex} - [k_M + k_{MD}([D]_0 - [^1D^*])] \times [^1M^*] - \gamma_{MM}[^1M^*]^2 - \gamma_{MD}[^1D^*][^1M^*] - \gamma_{MT}[T_1][^1M^*] \quad (10)$$

As before we ignore the S-T annihilation based on the low concentration of triplets. Because of the quadratic dependence on  $[^1M^*]$ , the general steady-state solution of (10) is awkward. In the limit that the heterogeneous annihilation process (i.e.,  $^1D^* - ^1M^*$ ) dominates the kinetics then

$$[^1M^*]_{ss} = (1 - f)I_{ex} / (\gamma_{MD} - k_{MD})[^1D^*]_{ss} \quad (11)$$

but this inverse dependence on  $[^1D^*]_{ss}$  (i.e., monomer fluorescence inversely proportional to excimer fluorescence) is never observed. If homogeneous annihilation dominates then

$$[^1M^*]_{ss} = ((1 - f)/\gamma_{MM})^{1/2} I_{ex}^{1/2} \quad (12)$$

This dependence is very close to what is observed and so we assume that homogeneous annihilation is the most important biphotonic process that affects the  $^1M^*$  state. Substituting eq 12 into the  $[^1D^*]_{ss}$  expression (eq 8) further emphasizes that while the  $I_{ex}$  dependence of  $[^1D^*]_{ss}$  is complicated,  $[^1D^*]_{ss}$  should have a tendency to approach saturation at high  $I_{ex}$  values.

The assumed kinetic equation for  $[T_1]$  is

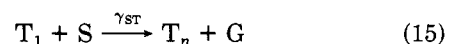
$$d[T_1]/dt = k_{MT}[^1M^*] + k_{DT}[^1D^*] - k_T[T_1] - \gamma_{MT}[^1M^*][T_1] - \gamma_{DT}[^1D^*][T_1] \quad (13)$$

T-T annihilation is ignored because of the low overall concentration of the  $T_1$  state. At low  $I_{ex}$  the steady-state triplet concentration should be proportional to  $I_{ex}$  so long as  $[^1M^*]_{ss}$  and  $[^1D^*]_{ss}$  are proportional to  $I_{ex}$ . If the annihilation terms  $\gamma_{MT}[^1M^*]$ ,  $\gamma_{DT}[^1D^*]$  are much larger than  $k_T$  then

$$[T_1]_{ss} = (k_{MT}[^1M^*]_{ss} + k_{DT}[^1D^*]_{ss}) / (\gamma_{MT}[^1M^*]_{ss} + \gamma_{DT}[^1D^*]_{ss}) \quad (14)$$

Obviously this expression begins to saturate faster than  $[^1M^*]_{ss}$  and is qualitatively similar to eq 8 for  $[^1D^*]_{ss}$ . However, there is no feature in eq 14 that indicates the decrease of  $[T_1]_{ss}$  with  $I_{ex}$  at the highest laser intensity nor the fact that this effect depends on the molecular weight of the polymer. We speculate that this observation reflects the statistics of polymer coil excitation. S-T annihilation requires the simultaneous existence of a  $T_1$  state and either  $^1M^*$  or  $^1D^*$  on the same polymer coil. The probability of multiple excitation of a coil increases with the number of chromophores/coil. The fact that the classical result (eq 14) does not reflect these "statistical effects" is a limitation in the application of homogeneous kinetics to an inherently inhomogeneous system.

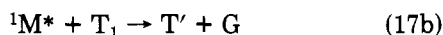
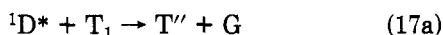
We should comment further about S-T annihilation. Since this process can occur via a Förster process, it may be written (see eq 7)



where  $T_n$  is a higher triplet state. For the Förster transfer to be maximized the S fluorescence should overlap extensively with  $T_1 - T_n$  absorption. By this criterion and for the polymers studied the bimolecular rate constant  $\gamma_{DT}$  should be larger than  $\gamma_{MT}$  and  $\gamma_{DT}^{P2VN} < \gamma_{DT}^{P4VBP}$ . Since the  $T_n$  state can return to  $T_1$  by radiationless decay the quantum efficiency of the S-T annihilation channel must be considered. If a steady-state approximation is made for  $[T_n]$ , then the steady-state solution to the modified equation for  $[T_1]_{ss}$  is

$$[T_1]_{ss} = (k_{MT}[^1M^*]_{ss} + k_{DT}[^1D^*]_{ss}) / (k_T + \gamma_{MT}(1 - \Phi_{TT'})[^1M^*]_{ss} + \gamma_{DT}(1 - \Phi_{TT''})[^1D^*]_{ss}) \quad (16)$$

where  $\Phi_{TT'}$  and  $\Phi_{TT''}$  are the quantum yields of  $T' \rightarrow T_1$  and  $T'' \rightarrow T_1$ , respectively, and  $T'$  and  $T''$  are the triplet states reached by the Förster processes



Thus in order to achieve saturation by this scheme,  $\Phi_{TT'}$  or  $\Phi_{TT''}$  must be significantly less than unity.

On the basis of the discussion above one expects that  $[T_1]_{ss}$  should be linear in  $I_{ex}$  at lower laser intensities and sublinear as  $I_{ex}$  is increased. For P4VBP we have observed that  $[T_1]$  is sublinear in  $I_{ex}$  at the lowest laser intensity for which  $OD_{TT}$  could be measured (see Figure 1b). This implies that S-T annihilation is very facile for this polymer. There are at least two factors that are expected to enhance S-T annihilation in P4VBP relative to P2VN:

(1)  $(\epsilon_{TT}^{P4VBP})_{max}$  is greater than  $(\epsilon_{TT}^{P2VN})_{max}$  by nearly a factor of 2 and  $\Phi_{fl}^{P4VBP}$  is greater than  $\Phi_{fl}^{P2VN}$  by a factor of 3. In both cases the  $^1D^*$  fluorescence overlaps the T-T absorption very well such that the S-T annihilation process should involve primarily the  $^1D^*$  state. Therefore for S-T annihilation to be important there must exist simultaneously on the polymer coil the  $^1D^*$  state and the  $T_1$  state.

(2) The two precursor states of  $T_1$  are  $^1M^*$  and  $^1D^*$ . If we assume that the intersystem crossing quantum yield for  $^1M^*$  is decreased in the polymer relative to the model compound according to

$$\Phi_{isc}^{polym}(^1M^*) = \Phi_{isc}^{model}(k_M^{model}/k_M^{polym}) \quad (18)$$

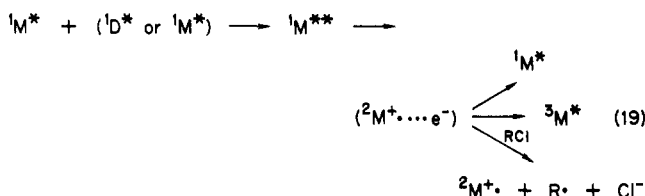
then we estimate<sup>17</sup>  $\Phi_{isc}^{P4VBP}(^1M^*) \sim 0.09-0.15$  and  $\Phi_{isc}^{P2VN}(^1M^*) \sim 0.02$ . The importance of these estimates is the following:  $T_1$  states with a  $^1M^*$  precursor are present on the same time scale as the  $^1D^*$  state appears. On the other hand  $T_1$  states with a  $^1D^*$  state precursor appear on the same time scale as the  $^1D^*$  state decays. Thus the higher the value of  $\Phi_{isc}^{polym}(^1M^*)$  the more important  $^1D^*-T_1$  annihilation will be.

Thus we submit that these two factors taken together are the reason for the relative importance of S-T in P4VBP. On the basis of the observed sublinear dependence of  $[T_1]_{ss}$  on  $I_{ex}$  it would seem that on the average a polymer coil that has one pendent biphenyl in the  $T_1$  state must have at least one  $^1D^*$  excited state simultaneously.

One of the surprising observations we have made in this study is the decreased  $T_1$  formation for the polymers at higher laser intensities if the solvent is  $CH_2Cl_2$  with concomitant formation of the radical cation. This phenomenon is completely absent in naphthalene or 4-methylbiphenyl and is present to only a slight extent in dinaphthylpropane (see Figure 4). The  $I_{ex}$  dependence of  $^1M^*$  and  $^1D^*$  fluorescence was essentially the same for MTHF and  $CH_2Cl_2$  (see Figure 5), and the steady state quantum yields (at low  $I_{ex}$ ) and fluorescence lifetimes are

essentially the same for these two solvents.

Thus it seems reasonable that the solvent dependence we observe is the result of the solvent interacting with the  $^1M^{**}$  state produced from S-S annihilation (eq 2a). We postulate the following:



The reaction represented in eq 19 is an elaboration of that in eq 2. In principle the ion pair  $({}^2M^+ \dots e^-)$  could be either a geminate pair or a dissociated electron-ion pair (depending on solvent and/or the energy of the  $^1M^{**}$  state). The degree of electron-ion separation can also determine the yields of singlet and triplet excited states.<sup>18</sup> A number of solvents, including  $CH_2Cl_2$ , are known to be able to trap solvated electrons, and in the case of alkyl halides the final product is an alkyl radical and halide ion.<sup>19</sup> Thus the present results provide two examples of biphotonic chemistry that is only important for polymers and which can be directed by the choice of solvent.

Up to now most of the discussion has focused on the annihilation processes in the kinetics of the polymer systems which in turn are responsible for the inverse molecular weight effect and large reduction in triplet quantum yield ( $\Phi_{isc}$ ). Yet, as can be seen in Table I, the values of  $\Phi_{isc}$  for both P2VN and P4VBP in the limit of low excitation energy are about five times lower than their monomeric model compounds. This would suggest that excimer formation lowers  $\Phi_{isc}$  for naphthalene and biphenyl compounds, such that one would expect a proportionality between the excimer to monomer fluorescence ratio and  $\Phi_{isc}$ . However, this does not seem to be the case for P2VN and its dimeric model compound, DNP. The  $\Phi_{isc}$  value of DNP is approximately 3.5 times that of P2VN-1 even though the excimer to monomer ratio is essentially identical for these two molecules. The following argument accounts for a part of the difference in  $\Phi_{isc}$  for P2VN and DNP. Zachariasse et al.<sup>20</sup> have studied various bichromophoric compounds in which they have determined the various photophysical rates involving the excited monomer and excimer states for DNP. They report an excimer lifetime of 86 ns while that for P2VN as determined by us is 45 ns in  $CH_2Cl_2$ . The difference in lifetimes could be due to the increased crowding of chromophores in P2VN which serves to enhance internal conversion processes in P2VN relative to DNP. (A similar observation was made for P1VN.<sup>4</sup>) If the intersystem crossing rate from the singlet excimer to the lowest triplet is the same from P2VN and DNP, then the expected quantum efficiency of triplet formation from the excimer state for P2VN would be approximately half that of DNP. Since a large fraction of excitation energy resides in the excimer state for both P2VN and DNP, this argument would account for at most a factor of 2 difference in  $\Phi_{isc}$  between P2VN and DNP. Another factor that may influence  $\Phi_{isc}$  is the rate of excimer dissociation, but we do not have enough data for P2VN to make a comparison with DNP.

We do not have available to us a bichromophoric model compound for P4VBP, but like P2VN the value of  $\Phi_{isc}^{P4VBP}$  is smaller than its monomeric model compound. One noticeable difference between the naphthalenic compounds and P4VBP is that  $\Phi_{fl}^{P4VBP}$  increases with excimer formation. This has been observed before by Zachariasse et al.<sup>20</sup> for dibiphenylpropane and for P4VBP by Albuin et

al.<sup>21</sup> This behavior has been ascribed to the nonparallel configuration of the biphenyl excimer which leads to a larger radiative rate for the excimer relative to excimers in a parallel, sandwich configuration (e.g., naphthalene and pyrene). Thus, the probable reason for the reduction of  $\Phi_{isc}$  upon excimer formation in P4VBP is the enhanced rate of internal conversion and fluorescence from the excimer state.

### Summary

The previous report<sup>1</sup> of an inverse molecular weight effect and large reduction in  $\Phi_{isc}$  for P2VN has been found to be the result of intracoil singlet-singlet annihilation. From our study it is clear that the lowest possible excitation intensity must be used in the measurement of  $\Phi_{isc}$  for polymer systems so as to minimize any singlet-singlet or other excited-state annihilation processes. Another factor that decreases  $\Phi_{isc}$  for P4VBP and P2VN is the diminished quantum efficiency of intersystem crossing from the singlet excimer to the lowest triplet state.

A kinetic scheme that incorporates a finite degree of heterogeneity in the description of the kinetics of the excited state of the polymer has been used to describe the intensity dependencies seen in the fluorescence and transient absorption of the polymer systems. The kinetic model, although oversimplified, is able to rationalize most of the features of the data for excitation intensities such that annihilation processes dominate the decay kinetics.

Finally, a novel discovery of enhanced photoionization in poly(vinylaromatic) solutions in  $\text{CH}_2\text{Cl}_2$  at high laser intensities has been reported. It is believed that this photoionization is the result of singlet-singlet annihilation reaction occurring within the polymer chain. This annihilation results in a highly excited singlet state which donates an electron to the  $\text{CH}_2\text{Cl}_2$  solvent. After capturing an electron the alkyl halide solvent undergoes a dissociative attachment reaction to form a neutral radical and a chloride ion that eventually protects the radical cation from the recombination reaction with the electron.

**Acknowledgment.** We acknowledge the financial support of the Robert A. Welch Foundation (Grant F-356) and the National Science Foundation (Grant DMR-8013709). We acknowledge the help of the staff and facilities of the Center for Fast Kinetics Research which is jointly supported by the Biotechnology Branch of the Division of Research Resources of the National Institutes of Health (Grant RR00886) and the University of Texas at Austin. We acknowledge helpful comments on this paper by H. Masuhara.

### Appendix. Analysis of the Two-State Model of Scheme I

It is often observed that the decrease in  $\Phi_M^f$  (monomer fluorescence quantum yield) in a polymer is not consistent with the ratio of fluorescence lifetimes ( $\tau_M^{\text{polym}}/\tau_M^{\text{model}}$ ) and a simple Birks scheme (i.e., Scheme I without the  $^1\text{M}_D^*$  state). If we consider the steady-state solutions from Scheme I at low  $I_{ex}$  such that excited-state annihilation can be ignored (i.e., typical of spectrofluorimeters) then

$$[^1\text{M}_D^*]_{SS} = (fI_{ex})/k_{MD}^* \quad (\text{A-1})$$

$$\begin{aligned} [^1\text{M}^*]_{SS} &= ((1-f)I_{ex})/(k_M + k_{MD}[D]) \\ &= ((1-\Phi_{MD})(1-f)I_{ex})/k_M \end{aligned} \quad (\text{A-2})$$

$$\begin{aligned} [^1\text{D}^*]_{SS} &= (k_{MD}^*[^1\text{M}_D^*]_{SS} + k_{MD}[D][^1\text{M}^*]_{SS})/k_D \\ &= (f + (1-f)\Phi_{MD})(I_{ex}/k_D) \end{aligned} \quad (\text{A-3})$$

In eq A-2 and A-3

$$\Phi_{MD} = (k_{MD}[D])/(k_M + k_{MD}[D]) \quad (\text{A-4})$$

and  $k_M$  is the usual decay rate for the  $^1\text{M}^*$  state (i.e., it is assumed that the only difference between the model and the polymer  $^1\text{M}^*$  state is the excimer formation in the latter).

The steady-state concentration of the  $^1\text{M}^*$  state for the model compound is given by

$$[^1\text{M}^*]_{SS}^{\text{model}} = I_{ex}/k_M \quad (\text{A-5})$$

If the radiative rates of the  $^1\text{M}^*$  state for polymer and monomer are assumed to be equal, then the ratio of the  $^1\text{M}^*$  fluorescence intensity is

$$I_M^{\text{polym}}/I_M^{\text{model}} = (1-f)(1-\Phi_{MD}) \quad (\text{A-6})$$

The ratio of the fluorescence lifetimes is given by

$$\tau_M^{\text{polym}}/\tau_M^{\text{model}} = k_M/(k_M + k_{MD}[D]) = 1 - \Phi_{MD} \quad (\text{A-7})$$

so

$$(I_M^{\text{polym}}/I_M^{\text{model}})(\tau_M^{\text{model}}/\tau_M^{\text{polym}}) = 1 - f \quad (\text{A-8})$$

provides a very rough estimate of the number of initially excited singlet states that are nonfluorescent by virtue of very rapid excimer formation.

We have fit the total fluorescence of the polymers to a sum of monomer and excimer components and estimated the monomer fluorescence quantum yield ( $\Phi_M^f$ ) to be compared with the model compound fluorescent quantum yield ( $\Phi_M^{\text{model}}$ ) in eq A-8. If we use the value of  $\Phi_M^{\text{model}}$  and  $\tau_M^{\text{model}}$  for 2-methylnaphthalene (i.e.,  $\Phi_M^{2\text{-MN}} = 0.32$ ;  $\tau_M^{2\text{-MN}} = 59$  ns), then using the values for P2VN ( $\Phi_M^f = 0.01$ ,  $\tau_M^{\text{polym}} = 7.4$  ns) we obtain an  $f$  value of 0.75. Similarly for P4BVP,  $f$  is approximately 0.37 when 4-methylbiphenyl is assumed the model compound (i.e.,  $\Phi_M^{4\text{-MB}} = 0.17$ ,  $\tau_M^{4\text{-MB}} = 15.2$  ns and  $\Phi_M^f$  for P4VBP is 0.033,  $\tau_M^{\text{polym}} = 4.7$  ns). (If isopropylbiphenyl is taken as the model compound then  $f = 0.48$  is obtained.)

**Registry No.** P2VN, 28406-56-6; P4VBP, 25232-08-0; DNP, 14564-87-5; naphthalene, 91-20-3; 2-methylnaphthalene, 91-57-6; 4-methylbiphenyl, 644-08-6; biphenyl, 92-52-4.

### References and Notes

- Bensasson, R. V.; Ronfard-Haret, J. C.; Land, E. J.; Webber, S. E. *Chem. Phys. Lett.* **1979**, *68*, 438.
- (a) Masuhara, H.; Ohwada, S.; Mataga, N.; Itaya, A.; Okamoto, K.; Kusabayashi, S. *J. Phys. Chem.* **1980**, *84*, 2363. (b) Masuhara, H.; Tamai, N.; Inoue, K.; Mataga, N. *Chem. Phys. Lett.* **1982**, *91*, 109. (c) Masuhara, H.; Ohwada, S.; Seki, Y.; Mataga, N.; Sato, K.; Tazuke, S. *Photochem. Photobiol.* **1980**, *32*, 9.
- Lachish, U.; Williams, D. J. *Macromolecules* **1980**, *13*, 1322.
- Gupta, A.; Liang, R.; Maocanin, J.; Kliger, D.; Goldbeck, R.; Horwitz, J.; Miskowski, V. M. *Eur. Polym. J.* **1981**, *17*, 485.
- Pratte, J. F.; Webber, S. E. *Macromolecules* **1982**, *15*, 417.
- Pratte, J. F.; Webber, S. E. *J. Phys. Chem.* **1983**, *87*, 449.
- Pratte, J. F.; Webber, S. E. *Macromolecules* **1983**, *16*, 1188.
- Webber, S. E.; Avots-Avotins, P. E.; Deumie, M. *Macromolecules* **1981**, *14*, 105.
- Amand, B.; Bensasson, R. *Chem. Phys. Lett.* **1975**, *34*, 44.
- Bensasson, R.; Goldschmidt, C. R.; Land, E. J.; Truscott, T. G. *Photochem. Photobiol.* **1978**, *28*, 277.
- Berlman, I. B. "Handbook of Fluorescent Spectra of Aromatic Molecules", 2nd ed.; Academic Press: New York, 1971.
- See, for example: Lachish, U.; Shafferman, A.; Stein, G. *J. Chem. Phys.* **1976**, *64*, 4205.
- Irie, S.; Horii, H.; Irie, M. *Macromolecules* **1980**, *13*, 1355.
- Arai, S.; Ueda, H.; Firestone, R. F.; Dorfman, L. M. *J. Chem. Phys.* **1969**, *50*, 1072.
- Fredrickson, G. W.; Frank, C. W. *Macromolecules* **1983**, *16*, 572.
- Swenberg, C. E.; Webber, S. E. *Chem. Phys. Lett.* **1980**, *49*, 231.



- (17) The range of values cited is for 4-methylbiphenyl and 4-isopropylbiphenyl (ref 11) with the assumption  $\Phi_{isc} = 1 - \Phi_f$  (i.e., we neglect internal conversion).
- (18) Brockelhurst, B. *Nature (London)* 1969, 221, 921.
- (19) Hamill, W. H. "Radical Ions"; Kaiser, E. T., Kevan, L., Eds.; Interscience: New York, 1968; pp 321-416.
- (20) Zachariasse, K. A.; Kuhnle, W.; Weller, A. *Chem. Phys. Lett.* 1978, 59, 375.
- (21) Abuin, E.; Lissi, E.; Gargallo, L.; Radic, D. *Eur. Polym. J.* 1982, 18, 319.

## Photoluminescent Probes for Water-Soluble Polymers. Pressure and Temperature Effects on a Polyol Surfactant

Nicholas J. Turro\* and Chao-jen Chung†

Department of Chemistry, Columbia University, New York, New York 10027.

Received January 11, 1984

**ABSTRACT:** Five photoluminescent probes have been employed to investigate the behavior of a poly(ethylene oxide)-poly(propylene oxide) block copolymer in aqueous solution. The measured fluorescence probe parameters, at fixed probe concentration, were found to be dependent on the concentration of copolymers and to demonstrate a "low"-, "medium"-, and "high"-concentration domain. In the high-concentration domain the parameters were found to be extremely sensitive to temperature and pressure. The results are interpreted in terms of intramolecular and intermolecular micelle formation by the copolymer.

### Introduction

Water-soluble block copolymers with both hydrophobic and hydrophilic blocks (polyol surfactants) are expected to possess versatile properties characteristic of their amphiphilic structures.<sup>1</sup> Studies of macroscopic properties of polyol surfactants by bulk measurements (cloud point, surface tension, interfacial tension, foam height, etc.) have received extensive attention,<sup>2</sup> and structure and aggregation properties have been measured by light scattering and low-angle X-ray scattering.<sup>3</sup> Luminescence probes have provided a powerful method for the investigation of the structure and dynamics of micelles, polyelectrolytes, and other water-soluble macroaggregates<sup>4</sup> but to date have rarely<sup>5</sup> been employed to investigate polyols. Because of the potential similarity of aggregates formed by conventional micelles formed from detergent monomers and the aggregates formed by polyol surfactants, we have initiated photoluminescence probe investigations of water-soluble block copolymers of hydrophilic blocks of poly(ethylene oxide) and hydrophobic blocks of poly(propylene oxide).<sup>6</sup> The probes employed were pyrenecarboxaldehyde (PyCHO), a reporter of environmental micropolarity via shifts in its fluorescence maximum,<sup>7a</sup> [11-(3-hexyl-1-indolyl)undecyl]trimethylammonium bromide (6-In-11<sup>+</sup>), a reporter of environmental micropolarity via shifts in its fluorescence maximum<sup>7b</sup> and also a reporter of environmental microviscosity via loss of its fluorescence polarization,<sup>7c</sup> 1,3-di-( $\alpha$ -naphthyl)propane (DNP), a reporter of environmental micropolarity via measurements of the extent of intramolecular excimer formation<sup>7d</sup>, pyrene (Py), a reporter of aggregation numbers via its excimer fluorescence decay,<sup>7e</sup> and 1,3-bis(*N*-carbazolyl)propane (BCP), a reporter of environmental changes via excimer emission.<sup>7f</sup> In typical experiments, the fluorescence measurements were made and studied as a function of polymer concentration and then as a function of temperature or pressure at fixed polymer concentration.

### Experimental Section

PEO-PPO (0.8:1, catalog no. 16275, MW  $\approx$  3000, Polysciences, Inc.) was used without further purification.<sup>6</sup> PyCHO (Aldrich

Co.) was recrystallized from ethanol. The polymer is assumed to be of the A-B-A type (PEO-PPO-PEO), but its purity has not been established. The syntheses of 6-In-11<sup>+</sup> and DNP were described in the literature.<sup>8</sup> Pyrene (Aldrich Co.) was recrystallized from ethanol; BCP was prepared by a literature method.<sup>7f</sup> The emission spectra of PyCHO (excitation wavelength 380 nm), 6-In-11<sup>+</sup> (excitation wavelength 300 nm), and DNP (excitation wavelength 290 nm) were taken with a Perkin-Elmer MPF-3L or SLM system 4800 S subnanosecond spectrofluorometer. The decay of pyrene emission was taken with a single-photon-counting apparatus.<sup>9</sup> The pressure cell has been described previously.<sup>10</sup>

**Pyrenecarboxaldehyde (PyCHO).** The fluorescence emission maximum ( $\lambda_m^P$ ) of PyCHO has been shown to be very sensitive to its environment in homogeneous solutions.<sup>7a</sup> Under the assumption that the results from homogeneous solution can be applied to microheterogeneous systems, the fluorescence emission of PyCHO has been employed as a probe of micropolarity in micellar and other aggregates. The fluorescence maximum of PyCHO in aqueous solutions containing PEO-PPO<sup>6</sup> was investigated as a function of PEO-PPO concentration. Figure 1 summarizes the results of these studies. The solid curve shows a plot of  $\lambda_m^P$  for a fixed concentration of  $5 \times 10^{-5}$  M PyCHO. The magnitude of  $\lambda_m^P$  can be classified as having values characteristic of three regions: (1) a region at low polymer concentration (less than 0.1 g/dL) for which the value of  $\lambda_m^P$  is relatively constant and comparable to that of PyCHO in aqueous solution, (2) a region at higher concentrations (ca. 0.1-10 g/dL) for which the value of  $\lambda_m^P$  of PyCHO undergoes a significant blue shift as the polymer concentration is increased, and (3) a region at still higher polymer concentration (>10 g/dL) for which a further, sharper blue shift of  $\lambda_m^P$  occurs as the polymer concentration is increased.

**[11-(3-Hexyl-1-indolyl)undecyl]trimethylammonium Bromide (6-In-11<sup>+</sup>).** The fluorescence maximum ( $\lambda_m^I$ ) of 6-In-11<sup>+</sup> has been shown to be a monitor of microscopic polarity,<sup>7b</sup> and the loss of fluorescence polarization of 6-In-11<sup>+</sup> has been shown to be a monitor of microscopic viscosity.<sup>7c</sup> The variation of  $\lambda_m^I$  with PEO-PPO concentration was found to parallel the behavior of  $\lambda_m^P$  as shown in Figure 1. The magnitude of the loss of fluorescence polarization of In-6-11<sup>+</sup> was measured by conventional methods<sup>7c</sup> as a function of PEO-PPO concentration. The data were translated into microviscosity ( $\eta^I$ , units of cP) and the results are summarized in Figure 1. As was found for  $\lambda_m^P$  and  $\lambda_m^I$ , the values for  $\eta^I$  fall into three regions, with remarkably good correspondence of the  $\lambda_m$  and  $\eta^I$  methods.

**1,3-Di( $\alpha$ -naphthyl)propane (DNP).** The ratio of intramolecular excimer fluorescence emission to monomer fluorescence emission ( $I_e/I_m$ ) has been shown to be a monitor of microscopic viscosity<sup>7d</sup> in microheterogeneous media. The parameters  $I_e/I_m$  can be translated into microviscosities,  $\eta^N$ . The results of mea-

† Present address: Rohm and Haas Co., Research Laboratories, Spring House, PA 15477.